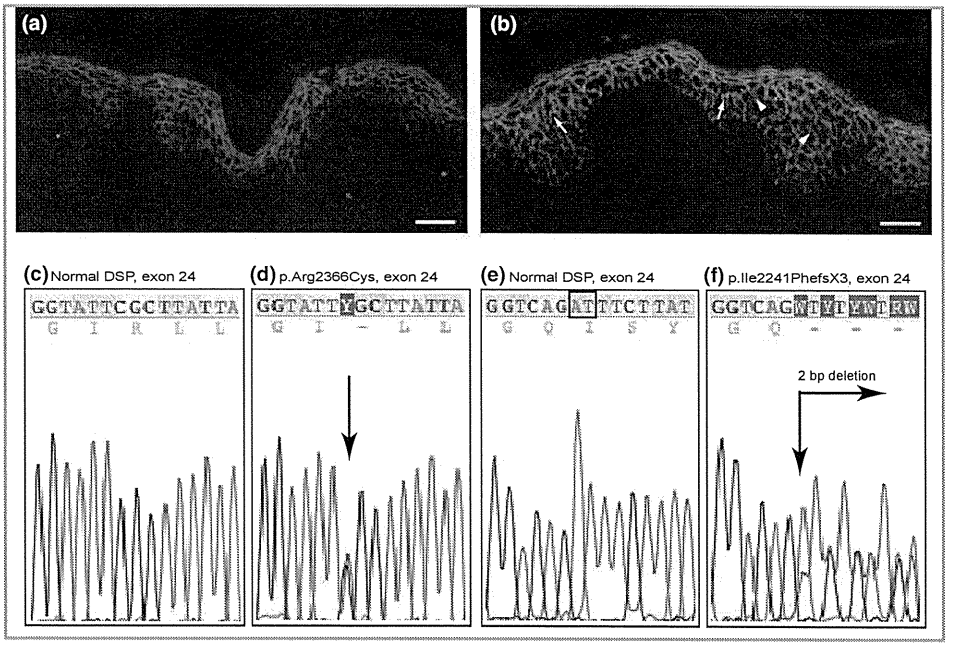

Fig 2. Immunofluorescence microscopy using an antibody against desmoplakin 1 and 2. (a) In normal control skin there was pan-epidermal staining at keratinocyte cell peripheries. (b) The patient's skin. In some cells there was occasional focal accentuation of staining at the cell periphery (arrows) and more cytoplasmic staining (arrowheads). Scale bars = 50 μm. (c–f) Molecular genetic analysis of the *DSP* gene showing compound heterozygous mutation. (c) Normal *DSP* sequence in exon 24, showing nucleotides 7090–7104. (d) The equivalent region as in (c) from the affected individual showing heterozygous missense mutation c.7096C>T (arrow) leading to amino acid substitution p.Arg2366Cys. (e) Normal desmoplakin sequence in exon 24, showing nucleotides 6715–6729. (f) The equivalent region as in (e) from the affected individual showing heterozygous two base-pair deletion mutation, c.6721–6722del (p.Ile2241Phefsx3, arrow), resulting in a premature termination codon six base pairs downstream.

References

1 Green KJ, Gaudry CA. Are desmosomes more than tethers for intermediate filaments? *Nat Rev Mol Cell Biol* 2000; **1**:208–16.

2 Lai-Cheong JE, Arita K, McGrath JA. Genetic diseases of junctions. *J Invest Dermatol* 2007; **127**:2713–25.

3 Whittock NV, Ashton GH, Dopping-Hepenstal PJ *et al.* Striate palmoplantar keratoderma resulting from desmoplakin haploinsufficiency. *J Invest Dermatol* 1999; **113**:940–6.

4 Whittock NV, Wan H, Morley SM *et al.* Compound heterozygosity for non-sense and mis-sense mutations in desmoplakin underlies skin fragility/woolly hair syndrome. *J Invest Dermatol* 2002; **118**:232–8.

5 Cabral RM, Wan H, Cole CL *et al.* Identification and characterization of DSPIa, a novel isoform of human desmoplakin. *Cell Tissue Res* 2010; **341**:121–9.

6 Tanaka A, Lai-Cheong JE, Cafe ME *et al.* Novel truncating mutations in PKP1 and DSP cause similar skin phenotypes in two Brazilian families. *Br J Dermatol* 2009; **160**:692–7.

7 Mahoney MG, Sadowski S, Brennan D *et al.* Compound heterozygous desmoplakin mutations result in a phenotype with a combination of myocardial, skin, hair, and enamel abnormalities. *J Invest Dermatol* 2010; **130**:968–78.

8 Asimaki A, Syrris P, Ward D *et al.* Unique epidermolytic bullous dermatosis with associated lethal cardiomyopathy related to novel desmoplakin mutations. *J Cutan Pathol* 2009; **36**:553–9.

9 Al-Owain M, Wakeel S, Shareef F *et al.* Novel homozygous mutation in DSP causing skin fragility–woolly hair syndrome: report of a large family and review of the desmoplakin-related phenotypes. *Clin Genet* 2011; **80**:50–8.

10 Norgett EE, Lucke TW, Bowers B *et al.* Early death from cardiomyopathy in a family with autosomal dominant striate palmoplantar keratoderma and woolly hair associated with a novel insertion mutation in desmoplakin. *J Invest Dermatol* 2006; **126**:1651–4.

Funding sources: The work was funded by the Pachyonychia Congenita Project.

Conflicts of interest: none declared.

Genotype analysis in a patient with oculocutaneous albinism 1 minimal pigment type

DOI: 10.1111/j.1365-2133.2011.10690.x

MADAM, Oculocutaneous albinism (OCA) is a group of autosomal recessive hypopigmentary disorders affecting the skin, hair and eyes. The four known types of OCA (OCA1–4) are classified according to single-gene mutations in tyrosinase (TYR), P protein, tyrosinase-related protein 1 and solute carrier family 45, respectively.[1,2] OCA1 has been clinically divided into three types: A (OCA1A, MIM 203100), characterized by a complete lack of melanin throughout life due to the produc-

tion of an inactive TYR, B (OCA1B, MIM 606952), characterized by the development of some pigment in the hair and skin with time after 1–3 years due to a reduced activity of TYR,[1–3] and temperature-sensitive variants (OCA1TS) manifested as having depigmented body hairs, but with pigmented hairs in cooler regions of the body, such as the hands and feet, due to a temperature-sensitive TYR which is inactivated around 37 °C.[1–3]

A fourth clinical variant of OCA1 was proposed as minimal pigment type (OCA1MP) by King *et al.*[4] in 1986. It is characterized by only minimal activity of TYR and an accumulation of ocular pigment that increases with age. So far, nine cases of OCA1MP have been reported,[5] but no genotypic or molecular analyses have been done, although they have been performed in OCA1A, OCA1B and OCA1TS.

We report a patient with OCA1MP in whom we have clarified the *TYR* genotype leading to her OCA. We describe the results of chemical analyses of melanin contents of her hair and of functional analyses of the mutated *TYR* gene transfected into nonpigmented albino melanocytes.

This study was approved by the Ethics Committee of the Nagoya University Graduate School of Medicine, and was conducted according to the Declaration of Helsinki Principles of 1975, as revised in 1985. Informed written consent was obtained from the patient and from normal volunteers.

The patient was a 37-year-old Japanese woman with white skin, ivory white hair and grey irises. She had foveal hypoplasia, and melanin pigment in the fundi could not be recognized by clinical examination. She was almost blind but could appreciate light. She had no bleeding tendency. In childhood, she had white skin and hair, and blue irises with amblyopia. By middle age, several brown freckles had developed on the nape of her neck and on the backs of her upper arms, and those areas were easily damaged with sunlight (Fig. 1). Lesional skin biopsy from her right forearm revealed hyperpigmentation in the basal layer of the epidermis. 3,4-dihydroxyphenylalanine (DOPA) staining[6] was negative in the patient's hair bulbs.

The content of eumelanin and phaeomelanin in the hair of the patient was 86·4 ng mg^{-1} hair and 155 ng mg^{-1} hair, respectively, measured according to a method described previously.[7] It is remarkable that the phaeomelanin content of the patient with OCA1MP was almost the same as that obtained from four normally pigmented Japanese volunteers (mean ± SD 148 ± 28 ng mg^{-1}), and was twice that of a patient with OCA1A with homozygous mutations of p.R77Q (70 ng mg^{-1}). However, her eumelanin amount was far less than that of the volunteers (mean ± SD 14 640 ± 4069 ng mg^{-1}) and was almost the same as that of the patient with OCA1A (78·4 ng mg^{-1}). The hair of the patient with OCA1MP was actually ivory white, i.e. yellowish white, which may be due to the presence of phaeomelanin.

Mutation analysis, performed according to methods described previously,[2,8] revealed that the patient with OCA1MP had two missense mutations, p.R77Q and p.D383N, in her *TYR* gene, which had been reported for the first time

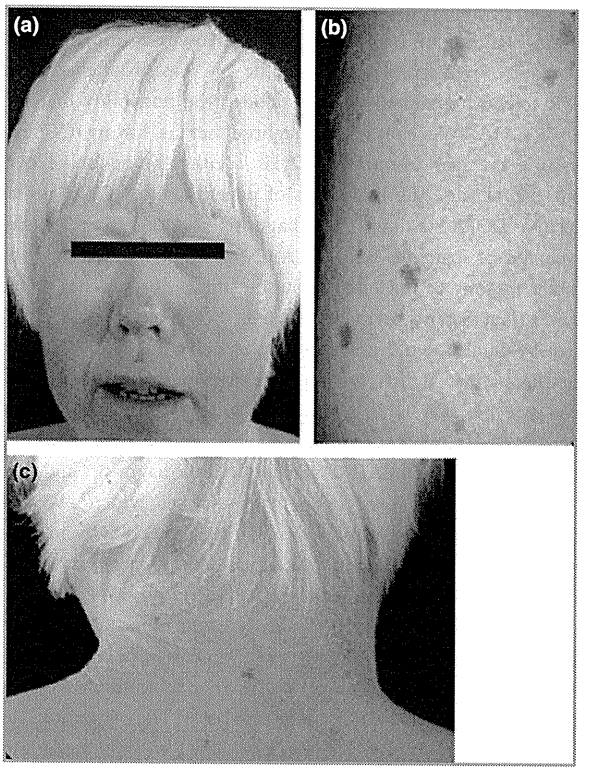

Fig 1. Clinical features: white skin, ivory white hair, grey irises (a) and brown freckles on the backs of the upper arms (b) and on the nape of the neck (c).

by Takeda *et al.*[9] and Spritz *et al.*[10] in 1990, and have been recognized in 12 of 83 (14%) and six of 83 (7%), respectively, of *TYR* genes of Japanese patients with OCA1 whom we have examined. Takeda *et al.*[9] had determined that the *TYR* gene with the mutation p.R77Q encoded a protein with no catalytic activity in a functional assay, i.e. amelanotic melanocytes transiently transfected with the p.R77Q mutated gene could produce no visible melanin.

We used a similar functional assay in this study to evaluate the ability of the mutant protein encoded by p.D383N *TYR* to produce melanin. About 73% of all melan-c melanocytes (kindly provided by Dr D.C. Bennett, Division of Basic Medical Sciences, St George's, University of London, U.K.) transfected with the wild-type *TYR* gene produced pigment, and the eumelanin and phaeomelanin contents in 10^6 cells were determined to be 48×10^3 and 360 ng, respectively. On the other hand, we could recognize no visible melanin deposition in albino melanocytes transfected with the p.D383N mutated gene or in those transfected with the p.R77Q mutated gene, from which RNA production was recognized by the method of reverse transcription–polymerase chain reaction. Further, we could not detect any eumelanin or phaeomelanin content, meaning that both types of melanin were below the sensitivity limits of our assays.

The patient initially appeared to have OCA1A, which is defined as the complete lack of TYR activity throughout life,

because of her white skin and hair from birth and the negative DOPA staining of her hair bulbs.[1–3] However, the development of brown freckles after middle age was proof that some TYR activity remained, which excluded the possibility that she has OCA1A. We could not diagnose her as having OCA1B, because the hair colour in OCA1B is either blond or yellow, and also because the hair bulbs of patients with OCA1B reveal positive DOPA staining.[1–3] A diagnosis of OCA1TS was easily excluded as patients with OCA1TS have pigmented hair in cooler regions of the body including the limbs and head, but our patient has no pigmented hair at her extremities.[1–3] Hermansky–Pudlak syndrome (HPS) was not a suitable diagnosis for our patient as that syndrome is known to be a TYR-positive type of OCA with a bleeding tendency due to a platelet storage pool defect.[1,2] After exclusion of OCA1A, OCA1B, OCA1TS and HPS, OCA1MP was the logical diagnosis, and that diagnosis was sustained by genetic analyses which revealed two missense mutations, p.R77Q and p.D383N, in the patient's *TYR* gene, but no mutation in other genes involved in OCA2, OCA3 and OCA4, as well as *HPS1* and *HPS4*.

Melanin synthesis starts from tyrosine due to the two catalytic activities of TYR, the hydroxylation of tyrosine to DOPA, and the oxidation of DOPA to dopaquinone, which then proceeds to eumelanogenesis.[7,11] The intermediate product, dopaquinone, can easily bind with cysteine to become cysteinyldopa which finally develops large polymers of phaeomelanin,[7,11] as shown in Figure 2. As Ito and Wakamatsu[11] previously discussed, cysteinyldopa formation can be carried out as long as the supply of cysteine remains. Therefore, it is reasonable that the faint TYR activity remaining in this patient with p.R77Q and p.D383N mutations of *TYR* could sustain phaeomelanogenesis to the same extent as in normally pigmented Japanese, but fail to proceed to eumelanogenesis.

As brown freckles developed in her sun-exposed areas and the histology was similar to that of solar lentigo, we suppose that they may have developed via the unknown pathomechanism that occurs in solar lentigines which often develop in healthy individuals.

King and coworkers[4,5] reported that OCA1MP clinically shows an accumulation of pigment only in the irises that increases with age. We would like to redefine it to any pigment accumulation requiring a long period of time in tissues such as the eye, the hair and lentigo.

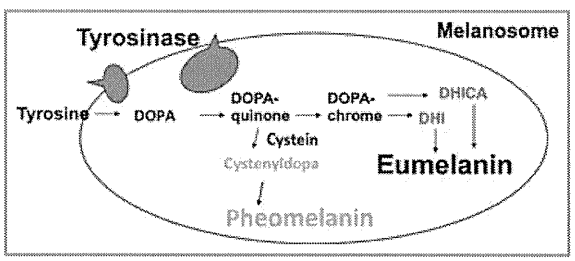

Fig 2. Biosynthetic pathways to eumelanin and phaeomelanin in melanosomes. Tyrosinase catalyses both tyrosine to 3,4-dihydroxyphenylalanine (DOPA) and DOPA to dopaquinone which then proceeds to eumelanogenesis in the absence of cysteine. In the presence of cysteine, dopaquinone binds exclusively with cysteine to become cysteinyldopa that proceeds to phaeomelanogenesis. DHI, 5,6-dihydroxyindole; DHICA, 5,6-dihydroxyindole-2-carboxylic acid.

Department of Dermatology, M. KONO
Nagoya University Graduate School of Medicine, T. KONDO
65 Tsurumai, Showa-ku, S. ITO
Nagoya 466-8550, T. SUZUKI*
Japan K. WAKAMATSU†
Department of Dermatology, S. ITO†
Yamagata University School of Medicine, Y. TOMITA
Yamagata, Japan
†*Department of Chemistry,*
Fujita Health University School of Health Sciences,
Toyoake, Japan
E-mail: miro@med.nagoya-u.ac.jp

References

1 Grønskov K, Ek J, Brondum-Nielsen K. Oculocutaneous albinism. *Orphanet J Rare Dis* 2007; **2**:43.
2 Tomita Y, Suzuki T. Genetics of pigmentary disorders. *Am J Med Genet C Semin Med Genet* 2004; **131C**:75–81.
3 King RA, Pietsch J, Fryer JP *et al.* Tyrosinase gene mutations in oculocutaneous albinism 1 (OCA1): definition of the phenotype. *Hum Genet* 2003; **113**:502–13.
4 King RA, Wirtschafter JD, Olds DP *et al.* Minimal pigment: a new type of oculocutaneous albinism. *Clin Genet* 1986; **29**:42–50.
5 Summers CG, King RA. Ophthalmic features of minimal pigment oculocutaneous albinism. *Ophthalmology* 1994; **101**:906–14.
6 Kugelman TP, Van Scott EJ. Tyrosinase activity in melanocytes of human albinos. *J Invest Dermatol* 1961; **37**:73–6.
7 Ito S, Wakamatsu K. Quantitative analysis of eumelanin and pheomelanin in humans, mice, and other animals: a comparative review. *Pigment Cell Res* 2003; **16**:523–31.
8 Miyamura Y, Verma IC, Saxena R *et al.* Establishment of tyrosinase sequence database in normally pigmented Indians and Japanese for rapid determination of novel mutations. *J Dermatol Sci* 2005; **39**:167–73.
9 Takeda A, Tomita Y, Matsunaga J *et al.* Molecular basis of tyrosinase-negative oculocutaneous albinism. A single base mutation in the tyrosinase gene causing arginine to glutamine substitution at position 59. *J Biol Chem* 1990; **265**:17792–7.
10 Spritz RA, Strunk KM, Giebel LB *et al.* Detection of mutations in the tyrosinase gene in a patient with type IA oculocutaneous albinism. *N Engl J Med* 1990; **322**:1724–8.
11 Ito S, Wakamatsu K. Chemistry of mixed melanogenesis – pivotal roles of dopaquinone. *Photochem Photobiol* 2008; **84**:582–92.

Funding sources: This work was supported by grants 18390312, 18659322 and 19390294 from the Ministry of Education, Science and Culture of Japan, and partially by The Cosmetology Research Foundation.

Conflicts of interest: none declared.

Accepted Date : 14-Mar-2012
Article type : OriginalArticle

A novel *IL36RN/IL1F5* homozygous nonsense mutation, p.Arg10X, in a Japanese patient with adult-onset generalized pustular psoriasis

K. Sugiura[1], T. Takeichi[1,2], M. Kono[1], Y. Ogawa[1], Y. Shimoyama.[3], Y. Muro[1], M. Akiyama[1]

Department of Dermatology[1], Department of Laboratory Medicine[3], Nagoya University Graduate School of Medicine
65 Tsurumai-cho, Showa-ku, Nagoya, Japan, 466-8550
Department of Dermatology, Inazawa City Hospital[2],
1-1 Gokusho-cho, Inazawa, Japan 492-8510

Corresponding Author: Kazumitsu Sugiura M.D., Ph.D.
Tel: +81-52-744-2318, Fax: +81-52-744-2318
E-mail: kazusugi@med.nagoya-u.ac.jp

Abbreviations: C-reactive protein (CRP), generalized pustular psoriasis (GPP), interleukin 36 receptor antagonist (IL36RN), palmoplantar pustulosis (PPP), psoriasis vulgaris (PV)

Keywords: adult onset, generalized pustular psoriasis, *IL36RN*, immunohistochemistry, nonsense mutation

Funding statement: None

Conflicts of interest: The authors have no conflicts of interest to declare.

Acknowledgements

This study was supported in part by a Grant-in-Aid for Scientific Research, (C) 23591617 (K.S.) from the Ministry of Education, Culture, Sports, Science and Technology of Japan and by a Grant-in-Aid for Scientific Research, (A) 23249058

(M.A.) from the Ministry of Education, Culture, Sports, Science and Technology of Japan.

Sir, Generalized pustular psoriasis (GPP) is a rare but severe form of psoriasis that is sometimes life threatening. It is characterized by sudden, repeated episodes of high-grade fever, generalized rash and disseminated pustules. The pathogenesis is unclear except for familial GPP, whose cause was recently identified as homozygous or compound heterozygous mutations in the *IL36RN* gene, also known as *IL1F5*, encoding the interleukin 36 receptor antagonist (IL36RN)[1, 2].

IL36RN is primarily expressed in the skin[3], and is an antagonist of three cytokines that belong to the interleukin-1 family: interleukin-36α, interleukin-36β, and interleukin-36γ, which are also known as interleukin-1F6, interleukin-1F8 and interleukin-1F9, respectively[4, 5]. These cytokines activate several proinflammatory signaling pathways, such as the nuclear factor-κB and mitogen-activated protein kinase pathways[6, 7].

We have followed a Japanese male patient with GPP, and *IL36RN* mutation analysis revealed the previously unreported homozygote nonsense mutation p.Arg10X.

A 68-year-old man presented with recurrent episodes of localized sterile pustules with erythema but without scaly erythematous plaques, on the extremities (Figure 1a, b) and the trunk, but not on the palmoplantar areas. He had been suffering from similar eruptions since the age of 34. He

once showed widespread generalized pustules accompanied by high fever and elevation of circulating CRP to 30 mg/dl, which were triggered by infection, and he was hospitalized. A skin biopsy from a pustular eruption on the trunk revealed a spongiform pustule of Kogoj in the epidermis (Figure 1c), which is consistent with GPP. He was diagnosed as GPP unassociated with psoriasis vulgaris (PV) or palmoplantar pustulosis (PPP). There was no apparent family history of skin disorders, although his parents are first cousins (Figure 1d).

The ethics committee of Nagoya University approved studies described below. The study was conducted according to the Declaration of Helsinki Principles. The participants gave written informed consent. The coding region of *IL36RN* (Gene bank accession No. 26525) was amplified from genomic DNA by PCR, as described previously[1]. Direct sequencing of the patient's PCR products revealed that the patient was homozygous for the previously unreported nonsense mutation of p.Arg10X (c.28C>T) in *IL36RN* (Figure 2a). C at nucleotide position 28 is 2 bases upstream from the C' end of exon 2 (the exon 2-intron 2 boundary) of *IL36RN*. *In silico* analysis by splicing donor score algorithm[8] was conducted to predict whether this mutation would lead to aberrant or normal splicing, and the results suggest that this mutation results in normal splicing (data not shown).

Immunohistochemistry with rabbit polyclonal anti-IL1F5 antibody (R&D Systems Inc. Minneapolis, MN) showed almost no expression of IL36RN in the patient's epidermal lesion but strong IL36RN expression in a positive control of psoriatic epidermis (Figure 2b,c), as reported previously[9]. Thus, it was apparent that the IL36RN protein was almost absent in the patient.

Very recently, *IL36RN* mutations were reported as causative genetic defects in GPP cases in Tunisian and European populations[1, 2]. In these reports, only three missense mutation were identified: *IL36RN,* i.e., IL36RN pLeu27Pro in the Tunisian population[1], and p.Arg48Trp and p.Ser113Leu in the European population[2]. pLeu27Pro and p.Ser113Leu were thought to be very prevalent mutations in the respective (Tunisian and European) populations.

We report for the first time a GPP patient with an *IL36RN* mutation in an Asian population, and we note that the mutation differs from those prevalent in the Tunisian and European populations. In addition, the present mutation is the first documented nonsense mutation of *IL36RN*. It is nearly a null mutation of IL36RN, and its abolition or extreme reduction of the protein expression of IL36RN was confirmed in the patient's skin. Thus, the present case bolsters the argument that IL36RN functional deficiency really contributes to GPP.

It is interesting that the disease onset of the present case was the rather late age of 34, although the present case was homozygous for *IL36RN* loss-of-function mutation and had no apparent IL36RN protein. In previous reports, most GPP cases with *IL36RN* mutations have been children, though they included three young adults (disease onset in the twenties). The only exceptional case in previous reports was a patient whose age of onset was 51[2]. The present case suggests that even when onset is not until middle age, we cannot exclude the possibility of underlying *IL36RN* mutations as causative genetic defects.

In addition, it is noteworthy that no GPP cases with *IL36RN* mutations, including the present case, have been associated with PV or PPP[1, 2], and the absence of PV and PPP is a clue in identifying GPP patients with *IL36RN* mutations.

We believe it is very important to discriminate familial GPP cases with *IL36RN* mutations from the other GPP cases, not only for genetic counseling but also because we expect familial GPP will be treatable with customized therapy that targets IL-36 signaling in the near future.

References

1. Marrakchi S, Guigue P, Renshaw BR, et al. (2011) Interleukin-36-receptor antagonist deficiency and generalized pustular psoriasis. N Engl J Med 365:620-8
2. Onoufriadis A, Simpson MA, Pink AE, et al. (2011) Mutations in IL36RN/IL1F5 are associated with the severe episodic inflammatory skin disease known as generalized pustular psoriasis. Am J Hum Genet 89:432-7
3. Mulero JJ, Pace AM, Nelken ST, et al. (1999) IL1HY1: A novel interleukin-1 receptor antagonist gene. Biochem Biophys Res Commun. 263:702-6.
4. Smith DE, Renshaw BR, Ketchem RR, et al. (2000) Four new members expand the interleukin-1 superfamily. J Biol Chem 275:1169-1175
5. Dinarello C, Arend W, Sims J, et al. (2010) IL-1 family nomenclature. Nat Immunol 11:973.
6. Debets R, Timans JC, Homey B, et al. (2001) Two novel IL-1 family members, IL-1 delta and IL-1 epsilon, function as an antagonist and agonist of NF-kappa B activation through the orphan IL-1 receptor-related protein 2. J Immunol 167:1440-6
7. Towne JE, Garka KE, Renshaw BR, et al. (2004) Interleukin (IL)-1F6, IL-1F8, and IL-1F9 signal through IL-1Rrp2 and IL-1RAcP to activate the pathway leading to NF-kappaB and MAPKs. J Biol Chem 279:13677-88
8. Sahashi K, Masuda A, Matsuura T, et al. (2007) In vitro and in silico

analysis reveals an efficient algorithm to predict the splicing consequences of mutations at the 5' splice sites. Nucleic Acids Res 35:5995-6003

9. Blumberg H, Dinh H, Trueblood ES, et al. (2007) Opposing activities of two novel members of the IL-1 ligand family regulate skin inflammation. J Exp Med 204:2603-14

Figure Legends

Figure 1. Skin manifestation, histopathology of the skin lesion and pedigree of the patient

Pustular erythema on internal left knee of the patient (a, b). Spongiosis of Kogoj and acanthosis are observed in the epidermis of the pustular erythema lesion in the trunk upon the patient's admission to hospital (c). Bar: 100 μm. Pedigree of the patient (d).

Figure 2. Sequence data of *IL36RN* and expression of IL36RN on the lesion of the GPP

Sequence data of *IL36RN* in the patient and control (a). Arrow shows heterozygous mutation of c. 28C>T (p.Arg10Ter). C at nucleotide position 28 is 2 bases upstream from the C' end of exon 2 (the exon 2-intron 2 boundary) of *IL36RN*. Immunohistochemistry of GPP lesion by anti-IL1F5 (IL36RN) (b). Staining was almost negative. Immunohistochemistry of skin lesion of a patient with psoriasis vulgaris by anti-IL1F5 (IL36RN) (c). Staining was strong in keratinocytes in the upper layers. Bar: 100 μm.

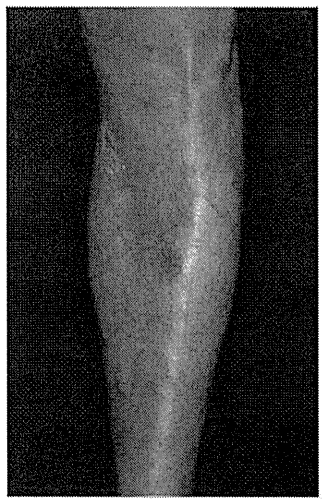

a

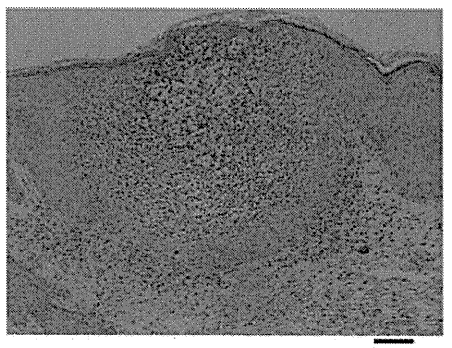

c

b

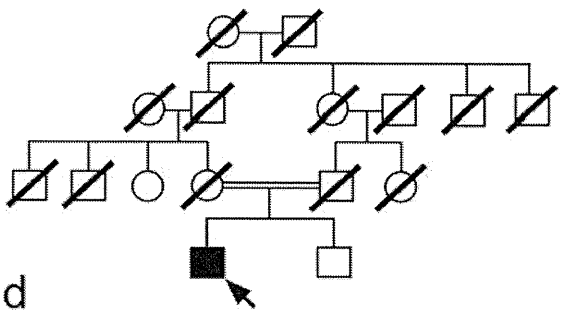

d

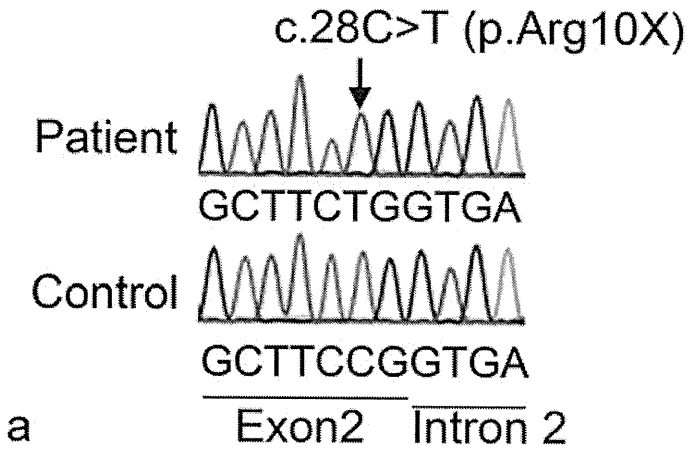
c.28C>T (p.Arg10X)
Patient
GCTTCTGGTGA
Control
GCTTCCGGTGA
Exon2
Intron 2

a

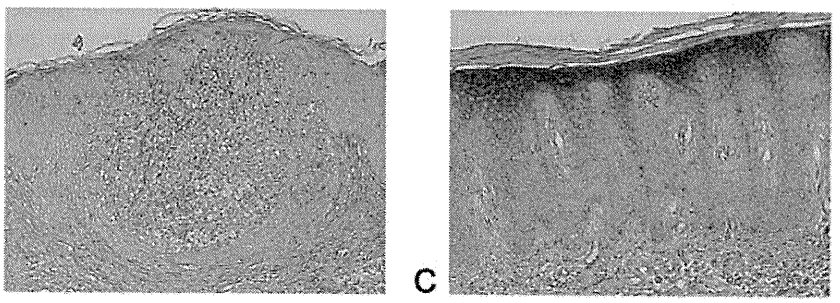

b c

IJD 5548 B
Journal Name | Manuscript No.
Dispatch: 4.4.12 | Journal: IJD | CE: GeethaPriya P.
Author Received: | No. of pages: 2 | PE: Prasanna
International Journal of Dermatology

Correspondence

Extraordinarily large, giant spider angioma in an alcoholic cirrhotic patient

Spider angioma/nevus, or nevus araneus, is a common cutaneous vascular anomaly, and is present in 10–15% of normal adults and children.[1] A spider angioma is typically a central, elevated, red punctum, from which blood vessels radiate 1–2 cm in diameter. We report here an extremely large spider angioma in a patient with liver cirrhosis.

A 68-year-old man with an 8-year history of alcoholic liver cirrhosis consulted our outpatient clinic complaining of a large reddish-purple soft tumor with radiating telangiectasia on the back. He had had the lesion for more than 1 year. The lesion had expanded and elevated gradually, and radiating telangiectasia appeared surrounding it. Subsequently, 10 or more small telangiectatic lesions appeared on his upper trunk and arms. He had been drinking about 50 g of alcohol per day until being diagnosed with liver cirrhosis. He had esophageal varices and was treated with endoscopic therapy. Physical examination revealed a reddish-purple, soft, dome-shaped node with a diameter of 2.3 × 1.3 cm, and telangiectasia radiating from the center to a diameter of 10 cm (Fig. 1).

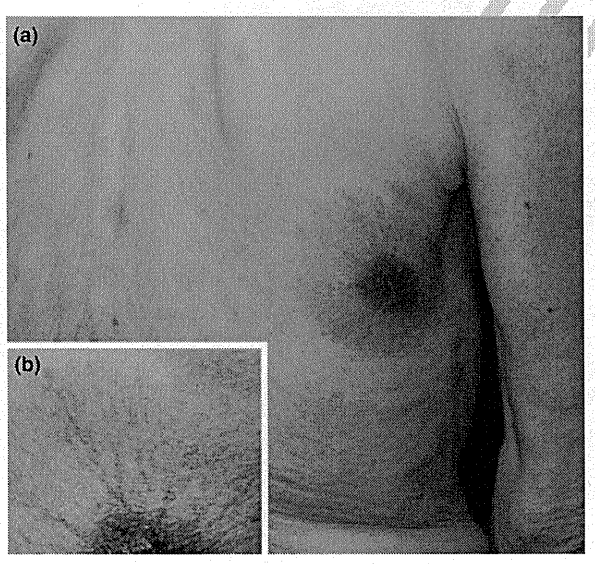

Figure 1 (a) A large reddish-purple soft tumor with radiating telangiectasia on the patient's back. (b) Close-up of the radiating telangiectasia. The clinical features of the present case are similar to those of a case reported previously[5]

Multiple, typical spider angiomas of ordinary size (<2 cm in diameter) were scattered on his upper trunk and upper extremities. Laboratory studies showed liver dysfunction and decreased platelet count. A skin biopsy was taken from the central reddish-purple node. Histopathologically, dilated vessels of various sizes were observed to have proliferated in the superficial and mid dermis. Inflammatory cells, mainly lymphocytes and histiocytes, were infiltrated around the dilated vessels, and erythrocyte extravasation was also seen. Endothelial cells of the vessels were round and protruding into the lumen, although no atypism was observed (Fig. 2). From these clinical and histopathological features, the diagnosis of spider angioma was made. During the 6-month follow-up period, no remarkable changes were seen in either the liver cirrhosis or the spider angioma. The patient did not want any treatment for the angioma.

Spider angioma is seen in patients with pregnancy, thyrotoxicosis, oral contraceptive use and, most commonly, liver cirrhosis. Spider angiomas are known to be more common in patients with alcoholic cirrhosis than in those with viral or idiopathic cirrhosis. The pathogenesis of spider angioma is still unclear. Li *et al.*[2] reported an association between elevated plasma levels of vascular endothelial growth factor and spider angiomas. In patients with non-alcoholic cirrhosis, the plasma level of substance P is elevated, and this may play an important

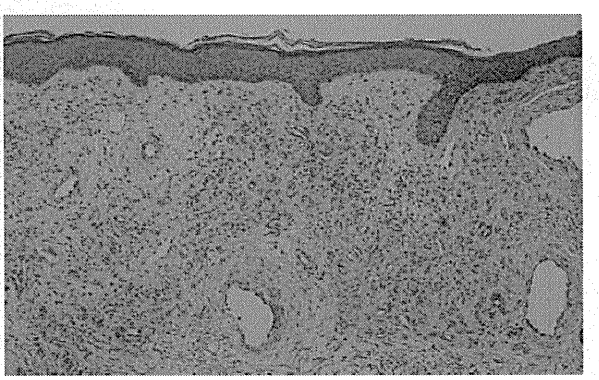

Figure 2 Photomicrograph of a skin biopsy specimen from the central node. Dilated vessels of various sizes are proliferated in the superficial and mid dermis. No atypism is observed in the endothelial cells. Low-density inflammatory cell infiltrate is observed around the dilated vessels (hematoxylin-eosin, original magnification ×100)

LOW RESOLUTION COLOR FIG

COLOR

role in the pathogenesis of spider angioma.[3] Estrogen also is suspected of playing a role.[4] Spider angiomas are usually <2 cm in diameter. Okada reported a giant spider angioma 6 cm in diameter.[5] As far as we know, the present spider angioma is the biggest ever reported. Generally, the central feeding vessel of spider angiomas can be destroyed with electrolysis or hyfrecation. Spider angiomas are also well treated by various types of lasers.[6,7] Giant spider angiomas can be treated by surgical excision.

The differential diagnosis for giant spider angioma includes several tumors of vascular origin, among them angiosarcoma, Kaposi's sarcoma and malignant hemangiopericytoma. Histopathological examination is often necessary to exclude these malignant tumors. Typical spider angiomas of ordinary size on the upper trunk and extremities were helpful in diagnosing the present case. Although giant spider angioma is rare, we have to keep it in mind in the differential diagnosis of large tumors of vascular origin, especially in patients with chronic liver diseases.

Hiroaki Hane, MD
Kenji Yokota, MD
Michihiro Kono, MD, PhD
Yoshinao Muro, MD, PhD
Masashi Akiyama, MD, PhD
Department of Dermatology, Nagoya University Graduate School of Medicine, Nagoya, Japan
E-mail: makiyama@med.nagoya-u.ac.jp

Funding: the authors have no funding sources for this work.

Conflicts of interest: the authors have no conflicts of interest to disclose.

doi: 10.1111/j.1365-4632.2012.05548.x

References

1 Requena L, Sangueza OP. Cutaneous vascular anomalies. Part I. Hamartomas, malformations, and dilation of preexisting vessels. *J Am Acad Dermatol* 1997; 37: 523–549; quiz 549–552.
2 Li CP, Lee FY, Hwang SJ, *et al.* Spider angiomas in patients with liver cirrhosis: role of vascular endothelial growth factor and basic fibroblast growth factor. *World J Gastroenterol* 2003; 9: 2832–2835.
3 Li CP, Lee FY, Hwang SJ, *et al.* Role of substance P in the pathogenesis of spider angiomas in patients with nonalcoholic liver cirrhosis. *Am J Gastroenterol* 1999; 94: 502–507.
4 Skafar DF, Xu R, Morales J, *et al.* Clinical review 91: female sex hormones and cardiovascular disease in women. *J Clin Endocrinol Metab* 1997; 82: 3913–3918.
5 Okada N. Solitary giant spider angioma with an overlying pyogenic granuloma. *J Am Acad Dermatol* 1987; 16: 1053–1054.
6 Dawn G, Gupta G. Comparison of potassium titanyl phosphate vascular laser and hyfrecator in the treatment of vascular spiders and cherry angiomas. *Clin Exp Dermatol* 2003; 28: 581–583.
7 Gupta G, Bilsland D. A prospective study of the impact of laser treatment on vascular lesions. *Br J Dermatol* 2000; 143: 356–359.

Author Query Form

Journal: IJD

Article: 5548

Dear Author,
During the copy-editing of your paper, the following queries arose. Please respond to these by marking up your proofs with the necessary changes/additions. Please write your answers on the query sheet if there is insufficient space on the page proofs. Please write clearly and follow the conventions shown on the attached corrections sheet. If returning the proof by fax do not write too close to the paper's edge. Please remember that illegible mark-ups may delay publication.

Many thanks for your assistance.

Query reference	Query	Remarks
1	AUTHOR: Figure 1 has been saved at a low resolution of 248 dpi. Please resupply at 300 dpi. Check required artwork specifications at http://authorservices.wiley.com/submit_illust.asp?site=1	

WILEY-BLACKWELL

USING e-ANNOTATION TOOLS FOR ELECTRONIC PROOF CORRECTION

Required software to e-Annotate PDFs: Adobe Acrobat Professional or Adobe Reader (version 8.0 or above). (Note that this document uses screenshots from Adobe Reader X)
The latest version of Acrobat Reader can be downloaded for free at: http://get.adobe.com/reader/

Once you have Acrobat Reader open on your computer, click on the Comment tab at the right of the toolbar:

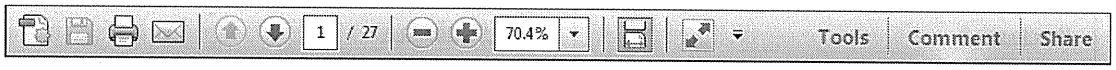

This will open up a panel down the right side of the document. The majority of tools you will use for annotating your proof will be in the Annotations section, pictured opposite. We've picked out some of these tools below:

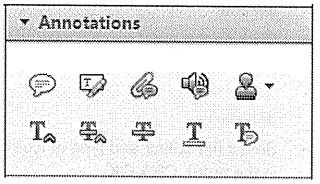

1. Replace (Ins) Tool – for replacing text.

Strikes a line through text and opens up a text box where replacement text can be entered.

How to use it

- Highlight a word or sentence.
- Click on the Replace (Ins) icon in the Annotations section.
- Type the replacement text into the blue box that appears.

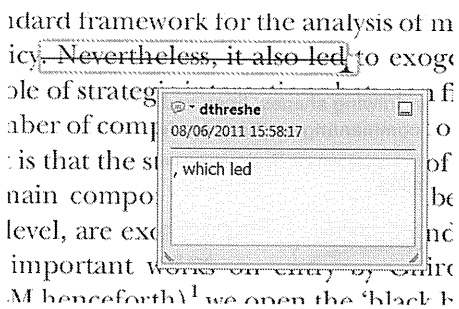

2. Strikethrough (Del) Tool – for deleting text.

Strikes a red line through text that is to be deleted.

How to use it

- Highlight a word or sentence.
- Click on the Strikethrough (Del) icon in the Annotations section.

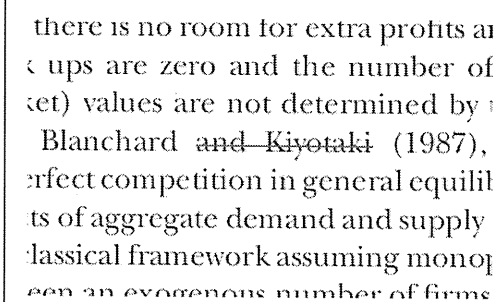

3. Add note to text Tool – for highlighting a section to be changed to bold or italic.

Highlights text in yellow and opens up a text box where comments can be entered.

How to use it

- Highlight the relevant section of text.
- Click on the Add note to text icon in the Annotations section.
- Type instruction on what should be changed regarding the text into the yellow box that appears.

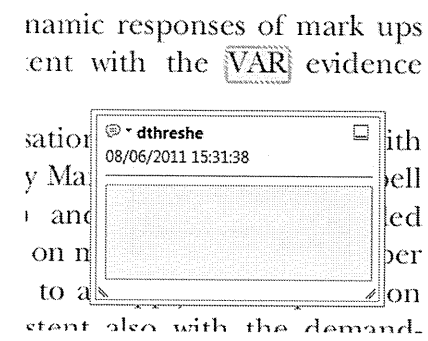

4. Add sticky note Tool – for making notes at specific points in the text.

Marks a point in the proof where a comment needs to be highlighted.

How to use it

- Click on the Add sticky note icon in the Annotations section.
- Click at the point in the proof where the comment should be inserted.
- Type the comment into the yellow box that appears.

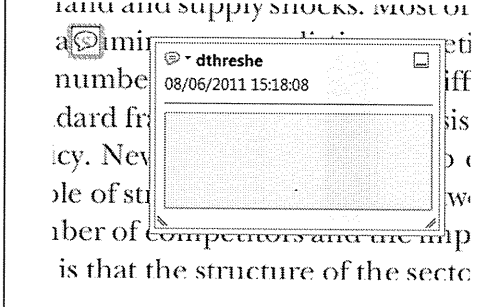

USING e-ANNOTATION TOOLS FOR ELECTRONIC PROOF CORRECTION

5. Attach File Tool – for inserting large amounts of text or replacement figures.

Inserts an icon linking to the attached file in the appropriate pace in the text.

How to use it

- Click on the Attach File icon in the Annotations section.
- Click on the proof to where you'd like the attached file to be linked.
- Select the file to be attached from your computer or network.
- Select the colour and type of icon that will appear in the proof. Click OK.

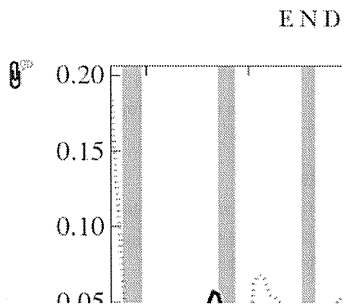

6. Add stamp Tool – for approving a proof if no corrections are required.

Inserts a selected stamp onto an appropriate place in the proof.

How to use it

- Click on the Add stamp icon in the Annotations section.
- Select the stamp you want to use. (The Approved stamp is usually available directly in the menu that appears).
- Click on the proof where you'd like the stamp to appear. (Where a proof is to be approved as it is, this would normally be on the first page).

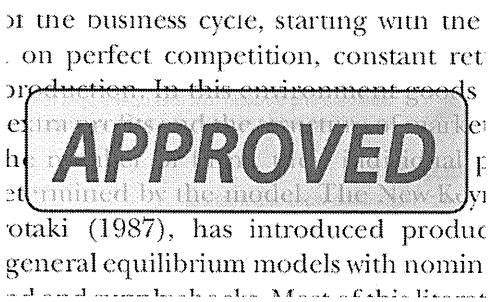

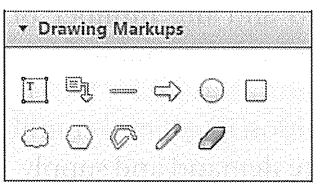

7. Drawing Markups Tools – for drawing shapes, lines and freeform annotations on proofs and commenting on these marks.

Allows shapes, lines and freeform annotations to be drawn on proofs and for comment to be made on these marks..

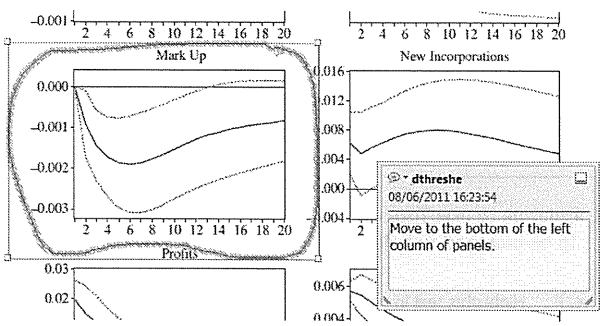

How to use it

- Click on one of the shapes in the Drawing Markups section.
- Click on the proof at the relevant point and draw the selected shape with the cursor.
- To add a comment to the drawn shape, move the cursor over the shape until an arrowhead appears.
- Double click on the shape and type any text in the red box that appears.

For further information on how to annotate proofs, click on the Help menu to reveal a list of further options:

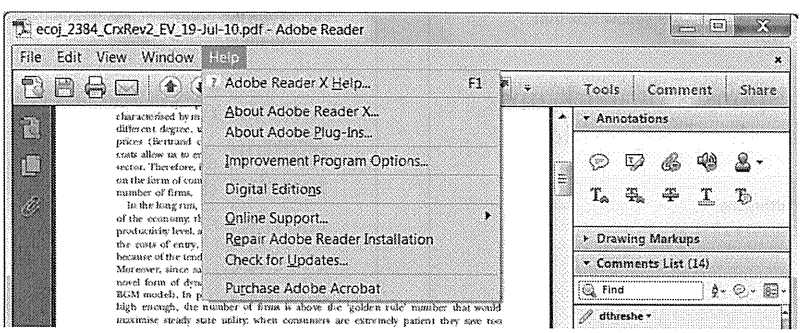

LEMD3 mutation to tropoelastin expression. *Eur J Dermatol* 2010; **20**:693–7.
8 Mumm S, Wenkert D, Zhang X *et al.* Deactivating germline mutations in LEMD3 cause osteopoikilosis and Buschke–Ollendorff syndrome, but not sporadic melorheostosis. *J Bone Miner Res* 2007; **22**:243–50.
9 Couto AR, Bruges-Armas J, Peach CA *et al.* A novel LEMD3 mutation common to patients with osteopoikilosis with and without melorheostosis. *Calcif Tissue Int* 2007; **81**:81–4.
10 Zhang Y, Castori M, Ferranti G *et al.* Novel and recurrent germline LEMD3 mutations causing Buschke–Ollendorff syndrome and osteopoikilosis but not isolated melorheostosis. *Clin Genet* 2009; **75**:556–61.
11 Baasanjav S, Jamsheer A, Kolanczyk M *et al.* Osteopoikilosis and multiple exostoses caused by novel mutations in LEMD3 and EXT1 genes respectively – coincidence within one family. *BMC Med Genet* 2010; **11**:110.
12 Yuste-Chaves M, Cañueto J, Santos-Briz A *et al.* Buschke–Ollendorff syndrome with striking phenotypic variation resulting from a novel c.2203C>T nonsense mutation in LEMD3. *Pediatr Dermatol* 2011; **28**:447–50.
13 Hellemans J, Debeer P, Wright M *et al.* Germline LEMD3 mutations are rare in sporadic patients with isolated melorheostosis. *Hum Mutat* 2006; **27**:290–6.
14 Lin F, Morrison JM, Wu W, Worman HJ. MAN1, an integral protein of the inner nuclear membrane, binds Smad2 and Smad3 and antagonizes transforming growth factor-beta signaling. *Hum Mol Genet* 2005; **14**:437–45.
15 Hinz B. Formation and function of the myofibroblast during tissue repair. *J Invest Dermatol* 2007; **127**:526–37.
16 Schiller M, Javelaud D, Mauviel A. TGF-beta-induced SMAD signaling and gene regulation: consequences for extracellular matrix remodeling and wound healing. *J Dermatol Sci* 2004; **35**:83–92.
17 Brown JJ, Bayat A. Genetic susceptibility to raised dermal scarring. *Br J Dermatol* 2009; **161**:8–18.

Funding sources: none.

Conflicts of interest: none declared.

Possible modifier effects of keratin 17 gene mutation on keratitis–ichthyosis–deafness syndrome

DOI: 10.1111/j.1365-2133.2011.10696.x

MADAM, Keratitis–ichthyosis–deafness (KID) syndrome (OMIM 148210, 242150) is a rare type of ectodermal dysplasia caused by mutations in the gap junction protein beta-2 gene (GJB2)[1] or beta-6 gene (GJB6).[2] On the other hand, mutations in genes encoding keratin 6a, 6b, 16 and 17 (*KRT6A*, *KRT6B*, *KRT16* and *KRT17*) are known to cause pachyonychia congenita (PC; OMIM 16720, 17210). PC and KID syndrome share similar symptoms, such as palmoplantar hyperkeratosis and onychodystrophy. This study reports a Japanese patient with atypical KID syndrome with the combined heterozygous mutations of a recurrent mutation in GJB2 and a novel mutation in the V1 region of KRT17.

The proband was a 40-year-old Japanese woman. She was the child of healthy, nonconsanguineous parents. From childhood, she had shown diffuse mutilating palmoplantar hyperkeratosis (Fig. 1a), nail dystrophy (Fig. 1b), hypotrichosis, sensorineural hearing loss, and vascularized keratitis. Periorificial hyperkeratosis was not seen. From these findings, the diagnosis of KID syndrome was made. She had had recurrent bacterial and fungal skin infections. In her twenties, painful tumours appeared on her lower limbs. In her thirties, tumours on both buttocks developed to take on a papilloma-like appearance (Fig. 1c). Etretinate with topical or systemic antibiotics and antifungal agents did not alleviate her symptoms. Skin abrasion was repeatedly conducted on the tumours. Histopathology of the lesions revealed epidermal pseudocarcinomatous hyperplasia with dilation of vessels in papillary and reticular dermis accompanied by mixed immune cell infiltrates, excluding the involvement of squamous cell carcinoma (Fig. 1d). Vacuolated keratinocytes, suggesting human papillomavirus infection, were not detected.

Genomic DNA extracted from peripheral blood was used as a template for polymerase chain reaction (PCR) amplification. Direct sequencing of *GJB2*, *GJB6*, *KRT6A*, *KRT6B*, *KRT16* and *KRT17* was performed as described elsewhere.[3–5] The medical ethical committee of Hokkaido University approved all the described studies. The study was conducted according to the Declaration of Helsinki Principles. The proband gave her written informed consent.

Mutation analysis of the proband's genomic DNA revealed a c.148G>A transition (p.Asp50Asn) in GJB2 (Fig. 2a), which is the most prevalent mutation in patients with KID syndrome.[1] Furthermore, the proband was found to be heterozygous for a c.177C>A transversion (p.Ser59Arg) in KRT17 (Fig. 2b). Restriction enzyme digestion of the PCR products by PvuII was carried out to confirm the c.177C>A in KRT17 (Fig. 2c). The c.177C>A in KRT17 was novel and was not detected in 200 alleles from 100 normal Japanese individuals. Mutation screening on the proband's parents could not be performed because the father was not alive and the mother did not consent. Keratin 17 (K17) immunohistochemistry on skin samples from several different sites revealed K17 expression in whole epidermis although its expression level did not vary between nonlesional and lesional skin specimens (data not shown).

As the clinical manifestations of the proband were atypical and more severe than those of other patients with KID syndrome – as evidenced, for example, by diffuse mutilating palmoplantar hyperkeratosis and recurrent granulation tissue formation on the buttock – we hypothesized that mutations in other genes might have affected the proband's phenotype through modifier effects. Modifier genes are defined as genes that affect the phenotypic expression of another gene, and several studies have demonstrated that modifier genes are involved in manifestations of inherited disorders.[6] *KRT6A*, *KRT6B*, *KRT16* and *KRT17*, the causative genes of PC, which affects the nails and the palmoplantar area, were selected as candidates for modifier gene investigation in our case, although we cannot exclude the possibility that there are some other genes which modify KID syndrome phenotype.

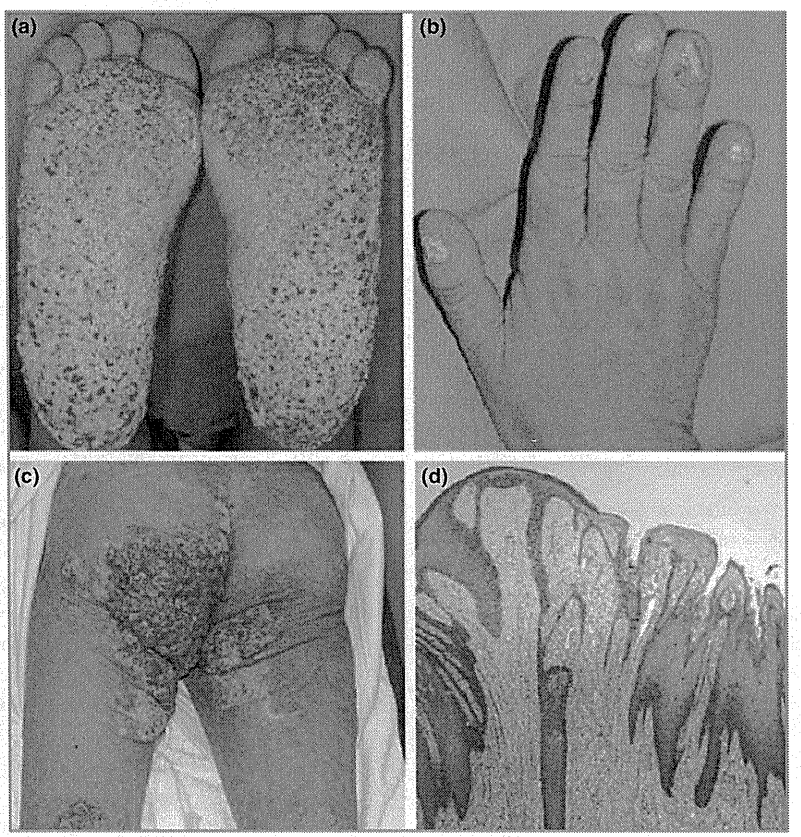

Fig 1. Clinical features of the proband. (a) Numerous erosive papules are coalesced into a hyperkeratotic plaque on the proband's soles. (b) Nail dystrophy is seen in the fingers. (c) A tumour is observed on the left buttock. Scars after skin abrasion are seen on the dorsal aspects of the thigh and on the right buttock. (d) Specimens from the tumour show pseudocarcinomatous hyperplasia of the epidermis. Dilated vessels with monocytic infiltrates are seen in the dermis (haematoxylin and eosin; original magnification × 100).

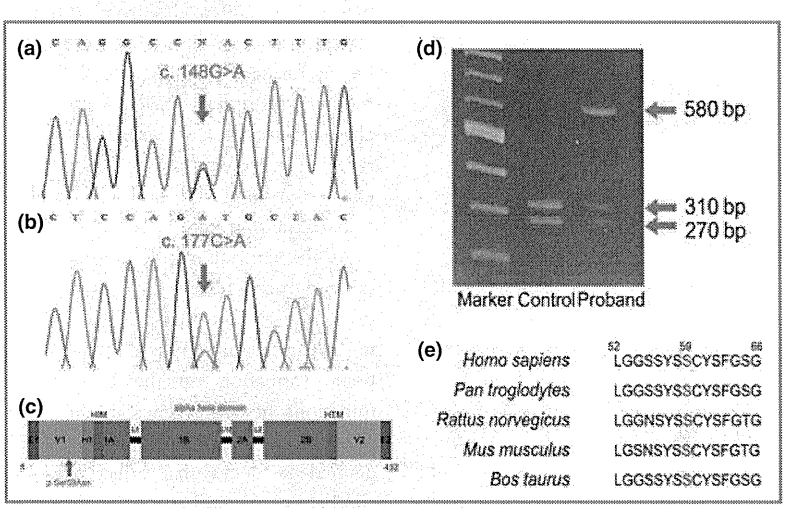

Fig 2. Mutation analysis. (a) The proband was heterozygous for a c.148G>A transition (p.Asp50Asn) mutation in *GJB2* (arrow). (b) c.177C>A (p.Ser59Arg) in *KRT17* was detected in the proband's genomic DNA (arrow). (c) PvuII restriction enzyme digestion of the polymerase chain reaction (PCR) products from genomic DNA of the proband and a normal control. c.177C>A resulted in the loss of a site for PvuII. PvuII restriction enzyme digestion of the PCR products from a normal controls reveals 270- and 310-bp bands. In contrast, 270-, 310- and 580-bp bands were detected in the proband, suggesting that she was heterozygous for c.177C>A. (d) A schematic of the structure of keratin 17. Note that Ser^{59} is located at the V1 region of the keratin molecule (arrow). HIM, helix initiation motif; HTM, helix termination motif. (e) Keratin 17 amino acid sequence alignment shows the level of conservation in diverse species of the amino acid Ser59 (red characters).

Most of the keratin mutations are within the helix boundary motifs, which are crucial for keratin monomers to form dimers and subsequent keratin networks.[7] The *KRT17* mutation found in the proband was located not within the helix boundary motifs but in the V1 region of K17 (Fig. 2d). In other keratin genes, such as *KRT5* and *KRT16*, some mutations have been reported within the V1 region, and the phenotypes resulting from these mutations are milder than those resulting from the mutations within the helix boundary motifs.[7] The V1 regions of keratin intermediate filament have glycine loops[8] and it has been suggested that these structures modulate flexibility and other unknown physical attributes of keratin filaments by interacting with similar structures in loricrin.[9] Ser^{59} is located within a highly conserved segment composed of the glycine loop in K17 (Fig. 2e). p.Ser59Arg in K17 is predicted to be probably damaging by PolyPhen-2, with a score of 0·893.[10]

Based on these findings, it is conceivable that the p.Ser59Arg variant in K17 has a modifying effect on the pathogenic *GJB2* mutation p.Asp50Asn and may contribute the proband's phenotype. Nevertheless, the limited scope of this study (single case report) does not allow us to determine the clinical significance of p.Ser59Arg in K17, and the influence of other genetic and epigenetic factors cannot be excluded.

*Department of Dermatology, Hokkaido University Graduate School of Medicine, North 15 West 7, Sapporo 060-8638, Japan
†Department of Dermatology, University of Miyazaki Faculty of Medicine, Miyazaki, Japan
‡Department of Dermatology, Nagoya University Graduate School of Medicine, Nagoya, Japan
E-mail: natsuga@med.hokudai.ac.jp

K. NATSUGA*
S. SHINKUMA*
M. KANDA*
Y. SUZUKI*
N. CHOSA†
Y. NARITA†
M. SETOYAMA†
W. NISHIE*
M. AKIYAMA*‡
H. SHIMIZU*

References

1 Mazereeuw-Hautier J, Bitoun E, Chevrant-Breton J *et al.* Keratitis–ichthyosis–deafness syndrome: disease expression and spectrum of connexin 26 (*GJB2*) mutations in 14 patients. *Br J Dermatol* 2007; **156**:1015–19.
2 Jan AY, Amin S, Ratajczak P *et al.* Genetic heterogeneity of KID syndrome: identification of a Cx30 gene (*GJB6*) mutation in a patient with KID syndrome and congenital atrichia. *J Invest Dermatol* 2004; **122**:1108–13.
3 Richard G, White TW, Smith LE *et al.* Functional defects of Cx26 resulting from a heterozygous missense mutation in a family with dominant deaf-mutism and palmoplantar keratoderma. *Hum Genet* 1998; **103**:393–9.
4 del Castillo I, Villamar M, Moreno-Pelayo MA *et al.* A deletion involving the connexin 30 gene in nonsyndromic hearing impairment. *N Engl J Med* 2002; **346**:243–9.
5 Kanda M, Natsuga K, Nishie W *et al.* Morphological and genetic analysis of steatocystoma multiplex in an Asian family with pachyonychia congenita type 2 harbouring a *KRT17* missense mutation. *Br J Dermatol* 2009; **160**:465–8.
6 Nadeau JH. Modifier genes in mice and humans. *Nat Rev Genet* 2001; **2**:165–74.
7 Szeverenyi I, Cassidy AJ, Chung CW *et al.* The Human Intermediate Filament Database: comprehensive information on a gene family involved in many human diseases. *Hum Mutat* 2008; **29**:351–60.
8 Steinert PM, Mack JW, Korge BP *et al.* Glycine loops in proteins: their occurrence in certain intermediate filament chains, loricrins and single-stranded RNA binding proteins. *Int J Biol Macromol* 1991; **13**:130–9.
9 Terrinoni A, Puddu P, Didona B *et al.* A mutation in the V1 domain of K16 is responsible for unilateral palmoplantar verrucous nevus. *J Invest Dermatol* 2000; **114**:1136–40.
10 Adzhubei IA, Schmidt S, Peshkin L *et al.* A method and server for predicting damaging missense mutations. *Nat Methods* 2010; **7**:248–9.

Funding sources: none.

Conflicts of interest: none declared.

Clinically manifest X-linked recessive ichthyosis in a female due to a homozygous interstitial 1·6-Mb deletion of Xp22.31

DOI: 10.1111/j.1365-2133.2011.10685.x

MADAM, X-linked recessive ichthyosis (XLI; OMIM 308100) is caused by mutations in or deletion of the entire *STS* gene coding for steroid sulfatase on Xp22.31.[1,2] Most patients (> 90%) have deletions, the most common one being approximately 1·6 Mb in size. The prevalence is about 1 : 1500 in males. The skin phenotype is fairly typical, consisting of mild erythroderma and generalized peeling or exfoliation of large, translucent scales within the first weeks after birth. Later, during infancy, large polygonal dark-brown scales develop on the extremities, trunk and neck. STS activity is reduced in female carriers, who can have dry skin in winter but otherwise have no recognizable phenotype. Three sisters with overt disease have previously been reported,[3] although without genetic analysis. We now describe a woman with clinically manifest XLI and elucidate the genetic basis.

The patient, of Dutch descent, presented to our department at the age of 18 years. She was born at term after prolonged delivery and, when she was a few weeks old, developed mild erythroderma with translucent scales that later on became larger and dark brown. Flexural areas were normal but she did have nuchal scaling. Her palms, soles and face were spared. There were no nail abnormalities, anosmia, or palmar hyperlinearity; psychomotor development was normal and she had no dysmorphic traits. Serum STS activity was zero. We diagnosed the patient as having XLI. The father, two of his brothers and several paternal first cousins also had been diagnosed with XLI. The same diagnosis had been established in several maternal uncles. Her mother and sister had dry scaling skin in the winter. We therefore surmised that XLI was segregating in both families.

In order to confirm the clinical diagnosis of XLI, fluorescent *in situ* hybridization (FISH) was carried out on metaphase